scientific reports

Check for updates

OPEN

# Microwave therapy promotes wound healing in diabetic mice by activating IL-33/ST2-mediated M2 macrophage polarization

Miaoxin He[1], Xinglan Huang[2], Tao Liu[1], Qian Yang[2], Yanfang Zheng[2], Yunxue Wu[2], Yanni Zhang[2], Yimin Liang[2], Zhongmin Liao[2], Shufen Peng[2], Hui Yin[1,3]✉ & Rongguo He[2]✉

**Chronic non-healing wounds are among the most common complications of diabetes, highlighting the urgent need for effective and accessible therapeutic strategies. Although microwave therapy has shown promise in promoting tissue repair, its underlying mechanisms in diabetic wound healing remain unclear. This study investigated the therapeutic effects of microwave therapy on diabetic wound healing and its potential modulation of the Interleukin-33 (IL-33) /ST2 signaling pathway. Full-thickness excisional wounds were established in C57BL/6 mice, categorized into normal control / wild-type (CON/WT), diabetic (DM), and ST2-deficient ($ST2^{-/-}$) groups. Mice received optimized microwave treatment (10 watts (W) for 10 min (min) daily), with or without IL-33-enriched macrophage supernatant (IL-33-MS). Wound healing outcomes were evaluated by histology, immunofluorescence, and gene expression analyses. In vitro experiments using RAW264.7 macrophages and HaCaT keratinocytes assessed IL-33 induction, macrophage polarization, and keratinocyte migration. Microwave treatment significantly accelerated wound healing in diabetic mice by enhancing granulation tissue formation, collagen remodeling, neovascularization, and myofibroblast activation. This effect was accompanied by increased IL-33 expression, particularly in macrophages, along with upregulation of M2 markers (*CD206*, *IL-4*, *YM1*) and downregulation of M1 markers (*iNOS*, *Tnf-α*). In $ST2^{-/-}$ mice, microwave therapy failed to promote wound repair, indicating that the IL-33/ST2 axis is essential for its pro-healing effect. IL-33-MS promoted wound closure in WT but not in $ST2^{-/-}$ mice. In vitro, microwave exposure upregulated IL-33 in macrophages and enhanced M2 polarization and HaCaT cell migration via ST2-dependent signaling. Microwave therapy facilitates diabetic wound healing by activating the IL-33/ST2 pathway, promoting M2 macrophage polarization, and improving the wound microenvironment. These findings provide mechanistic insight into the immunomodulatory effects of microwave therapy and support its potential as a non-invasive strategy for chronic diabetic wound management.**

**Keywords** Microwave therapy, IL-33/ST2 signaling, M2 macrophages, Diabetic wound healing, Immunomodulation

Diabetes is a chronic metabolic disease characterized by hyperglycemia resulting from insulin deficiency or resistance[1]. Its global prevalence continues to rise, with an estimated 540 million people affected in 2021 and projections indicating a further increase to 780 million by 2045[2]. Among the major complications, delayed wound healing poses a significant clinical challenge. Diabetic patients often suffer from impaired skin regeneration, leading to chronic non-healing wounds that may result in infections, amputations, or even death[3,4]. Conventional treatments, including debridement, pressure offloading, vascular improvement, and infection control, often yield limited results and are associated with technical complexity and potential side effects[5,6], underscoring the need for more effective and accessible therapeutic strategies.

[1] Guangdong Provincial Key Laboratory of Pharmaceutical Bioactive Substances, Guangdong Pharmaceutical University, Guangzhou 528405, China. [2]Department of Dermatology, Guangzhou Twelfth People's Hospital, 1 Tianqiang Road, Tianhe District, Guangzhou 510620, Guangdong, China. [3]Department of Microbiology and Immunology, Guangdong Pharmaceutical University, 280 Outer Ring East Road, University Town, Guangzhou 510006, Guangdong, China. ✉email: huiyin0103@163.com; 459363210@qq.com

Microwave physiotherapy has emerged as a promising physical modality for tissue repair due to its deep tissue penetration, non-ionizing energy, and adjustable parameters[7–10]. Previous studies have shown that microwave exposure can increase local temperature, enhance microcirculation, promote granulation tissue formation, and stimulate macrophage activity[7,11–13]. However, its mechanisms in diabetic wound repair remain poorly understood. Macrophages play a pivotal role in coordinating wound healing, transitioning from pro-inflammatory M1 to anti-inflammatory M2 phenotypes during tissue repair[3]. In diabetic conditions, this polarization process is often disrupted, leading to persistent inflammation and impaired healing[14,15]. Targeting macrophage polarization is therefore considered a potential therapeutic avenue for diabetic wounds.

IL-33, a member of the IL-1 cytokine family, functions as an "alarmin" secreted by keratinocytes and macrophages. By binding to its receptor ST2, IL-33 activates signaling pathways such as the PI3K/AKT, TGF-β, NF-κ B, and JAK/STAT, thereby inducing M2 polarization[16–20]. Recent studies have highlighted the IL-33/ST2 axis as a locally effective mechanism in diabetic wound repair[15,18,19,21–23]. Our previous work demonstrated that exogenous IL-33 promotes diabetic wound healing in mice by enhancing M2 macrophage activity and tissue regeneration[24]. Building upon these findings, this study investigates whether microwave therapy can facilitate diabetic wound repair by upregulating IL-33 expression and activating the IL-33/ST2 axis, thereby promoting macrophage polarization and modulating the wound microenvironment.

## Materials

### Experimental animals

Specific pathogen-free (SPF) male C57BL/6 mice, aged 6–8 weeks and weighing 20–25 g, were purchased from the Guangdong Experimental Animal Center (License No. SYXK [Yue] 2022 – 0125). SPF-grade ST2-deficient ($ST2^{-/-}$) male C57BL/6 mice of the same age and weight were obtained from Cyagen Biosciences Inc. (Guangzhou, China; License No. SCXK [Yue] 2013-0032). All animals were housed under SPF conditions at the Experimental Animal Center of Guangdong Pharmaceutical University with controlled humidity (40–60%), ambient temperature (21–25 °C), and a 12 h light/dark cycle. All experimental procedures were conducted in accordance with the Regulations on the Administration of Laboratory Animals of the People's Republic of China and institutional ethical guidelines. The animal ethics approval number is GDPULAC2024104. Meanwhile, the ARRIVE guidelines (https://arriveguidelines.org) were strictly followed in this study.

### Cell lines

RAW264.7 murine macrophage-like cells and immortalized human keratinocyte (HaCaT) cells were obtained from the American Type Culture Collection (ATCC, Manassas, VA, USA).

### Major reagents

Streptozotocin (Macklin, Shanghai, China); Purified anti-mouse CD31 (PECAM-1) antibody (Sino Biological, Beijing, China); Anti-α-SMA/ACTA2 antibody (Boster Biological, Wuhan, China); Anti-Collagen I antibody (Abcam, Cambridge, MA, USA); DAPI (Biosharp, Hefei, China); TRIzol™ Reagent (Invitrogen, Carlsbad, CA, USA); Anti-CD206/MRC1 antibody (Abmart, Shanghai, China); Cytokeratin 14/KRT14 antibody (Sino Biological, Beijing, China); F4/80 monoclonal antibody (Invitrogen, Carlsbad, CA, USA); iNOS polyclonal antibody (Proteintech, Wuhan, China); ST2/IL-1RL1 antibody (Sino Biological, Beijing, China); HiScript III All-in-One RT SuperMix Perfect for qPCR and ChamQ Universal SYBR qPCR Master Mix (Vazyme, Nanjing, China).

### qRT-PCR primers

Primers were designed using Primer Premier 5.0 software based on the gene sequences available in the NCBI GenBank. The forward and reverse primer sequences for each target gene are shown in Table 1.

| Gene | Upstream Primers(5'-3') | Downstream Primers(5'-3') |
|---|---|---|
| *Gapdh* | TTCACCACCATGGAGAAGGC | GGCATGGACTGTGGTCATGA |
| *IL-33* | CCTGCCTCCCTGAGTACATACA | CTTCTTCCCATCCACACCGT |
| *Tnf-α* | CTACTGCTTCAGCTCCACAG | TGCACTTGCAGGAGCGCAC |
| *Inos* | CAGCTGGGCTGTACAAACCT | CATTGGAAGTGAAGCGTTTCG |
| *IL-6* | TGGGGGAGATTCTCACTTTG | CCATCAGCGTTCCCATACTT |
| *IL-4* | GAGACTTCCATCCAGTTGCC | AAGTGCATCATCGTTGTTCAT |
| *YM1* | CATGAGCAAGACTTGCGTGAC | GGTCCAAACTTCCATCCTCCA |
| *Arg1* | GTCTGGCAGTTGGAAGCATC | TGGTTGTCAGGGGAGTGTTG |
| *Vegf* | GGACCCTGGCTTTACTGCTG | CACAGGACGGCTTGAAGATG |
| *vWF* | GGGGATGTCTGGACCTTGC | GTGACGATGTGCCGAGTGG |
| *Col3a1* | TCCCAGAAATCAACGAGAC | CATTTCCCACAGCCTTGAAT |
| *Fn1* | TGGAGATGCTCACTTTGACG | GCCTTGGCTGAGTGGTAGAG |

**Table 1**. The primers for the upstream and downstream regions of the genes.

## Experimental methods

### Establishment of wound model in normal mice

Thirty male C57BL/6 mice with comparable age and weight were anesthetized via intraperitoneal injection of 2% pentobarbital sodium (45 mg/kg). After shaving and disinfecting the dorsal skin with 75% ethanol, full-thickness excisional wounds (8 mm in diameter) were created under sterile conditions. Mice were randomly divided into five groups ($n=6$ per group): control group (CON) and four microwave treatment groups with different parameters (8 W 10 min, 10 W 10 min, 12 W 10 min, and 10 W 15 min). The CON group received no treatment. Microwave-treated groups received daily localized microwave therapy for 14 consecutive days. Wounds were photographed on days 1, 3, 5, 7, 9, 11, and 13, and wound area was measured using ImageJ software. Wound healing rate was calculated as:

$$Healing\ rate\ (\%) = \frac{(\text{Initial area} - \text{Current area})}{\text{Initial area}} \times 100\%$$

No mortality was observed during the course of the study, and all animals successfully completed the experimental cycle prior to being sacrificed for harvest.

### Diabetic mouse wound model

Twenty C57BL/6 mice were fasted for 12 h and then injected intraperitoneally with streptozotocin (STZ, 50 mg/kg) for five consecutive days. Blood glucose was measured on days 3, 5, and 7. Mice with glucose levels > 16.7 mmol/L and symptoms of polydipsia, polyphagia, and polyuria were considered successfully modeled. Based on parameter optimization experiments (see Fig. 1), 10 W for 10 min was determined as the optimal microwave setting. Mice were then randomly divided into two groups: DM group and DM + 10 W 10 min group. The latter received daily microwave treatment for 14 days; the DM group received no treatment. No mortality was observed during the course of the study, and all animals successfully completed the experimental cycle prior to being sacrificed for harvest.

### ST2-deficient mouse wound model

Ten C57BL/6 mice were used as the wild-type (WT) group, and twenty $ST2^{-/-}$ mice were randomly assigned to $ST2^{-/-}$ and $ST2^{-/-}$ + 10 W 10 min groups ($n=10$ per group). Full-thickness wounds were created as previously described. The $ST2^{-/-}$ + microwave group received daily 10 W 10 min microwave treatment for 14 days; other groups received no intervention. No mortality was observed during the course of the study, and all animals successfully completed the experimental cycle prior to being sacrificed for harvest.

### Wound tissue collection

At the end of the experiment, all mice were euthanized by cervical dislocation. Skin wound tissues were collected immediately after euthanasia. A portion of each wound tissue was fixed in 15% formaldehyde overnight for histological analysis, while the remaining tissue was processed for immunofluorescence, RT-PCR, and other molecular assays.

### H&E and masson's trichrome staining

On days 7 and 14 post-treatment, wound tissues were harvested, fixed in paraformaldehyde, and embedded in paraffin. Hematoxylin and eosin (H&E) staining was used to assess tissue architecture, and Masson's trichrome staining was performed to evaluate collagen deposition.

### Immunofluorescence staining

After deparaffinization and antigen retrieval, tissue sections were blocked and incubated overnight with primary antibodies. On the following day, secondary antibodies and DAPI were applied. Sections were mounted with anti-fade reagent and visualized under a fluorescence microscope. Signal intensity was quantified using ImageJ software.

### RAW264.7 cell culture and grouping

RAW264.7 cells were cultured and seeded into dishes. Cells were randomly divided into control and five microwave treatment groups (5 W 10 min, 8 W 10 min, 10 W 10 min, 8 W 5 min, 8 W 15 min). Supernatants from untreated macrophages (MS) and macrophages treated with the optimal microwave parameter (IL-33-MS) were collected and stored at − 80 °C.

### IL-33-MS combined microwave treatment in $ST2^{-/-}$ mice

Twenty WT and twenty $ST2^{-/-}$ mice were used to establish wound models and randomly assigned to four groups: MS group, IL-33-MS group, $ST2^{-/-}$ + MS group, and $ST2^{-/-}$ + IL-33-MS group. Each mouse received daily topical application of 50 μL of the corresponding supernatant for 14 days.

### HaCaT cell culture and microwave treatment

HaCaT cells were cultured and seeded into dishes, then randomly assigned to control and five microwave treatment groups (5 W 10 min, 8 W 10 min, 10 W 10 min, 8 W 5 min, 8 W 15 min). Treated cells were collected for subsequent analysis.

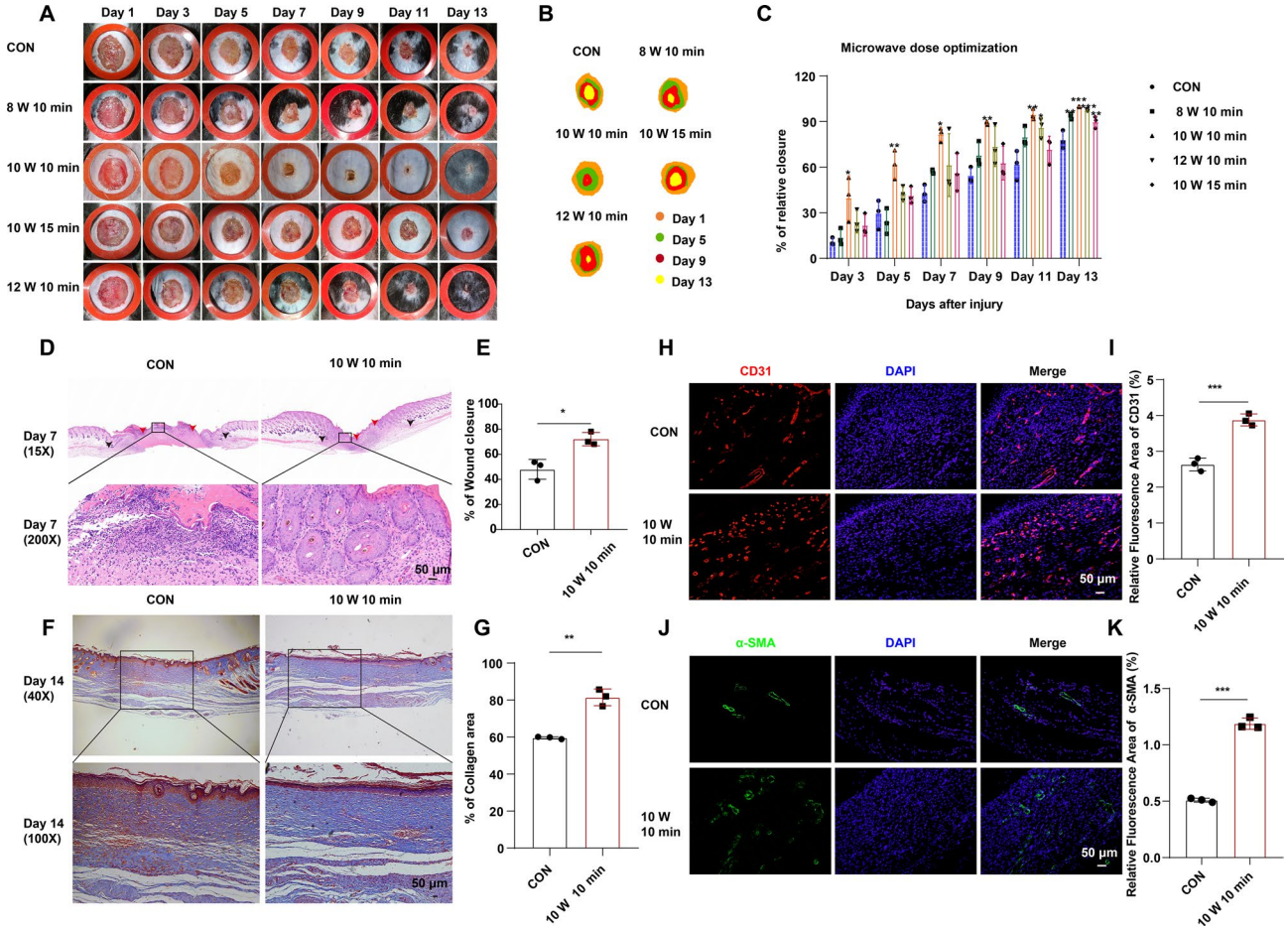


**Fig. 1**. Effects of microwave therapy on wound healing in normal mice. (**A**) Representative images of wound healing at days 1, 3, 5, 7, 9, 11, and 13 under different microwave treatment parameters. $n = 3$ per group. (**B**) Overlaid wound area outlines at each time point for all groups. (**C**) Quantitative analysis of wound closure rates over time. $n = 3$ per group. (**D**) H&E staining on day 7; black arrows indicate wound edges, red arrows indicate epidermal structure. (**E**) Quantification of epidermal regeneration rate. $n = 3$ per group. (**F**) Masson's trichrome staining on day 14. (**G**) Quantitative analysis of collagen volume fraction. $n = 3$ per group. (H) CD31 immunofluorescence staining (red) on day 7. (**I**) Quantification of CD31-positive fluorescence area. (**J**) α-SMA immunofluorescence staining (green) on day 7. (**K**) Quantification of α-SMA-positive fluorescence area. ( ns = not significant; $^{*}p < 0.05$; $^{**}p < 0.01$; $^{***}p < 0.001$).

## Immunofluorescence on coverslips

Cells were seeded onto coverslips, fixed after treatment, permeabilized, blocked, and then incubated sequentially with primary antibodies, secondary antibodies, and DAPI. The coverslips were mounted and observed under a fluorescence microscope.

## Scratch wound assay

HaCaT cells were cultured to approximately 90% confluence and then synchronized by incubation in serum-free medium for 2 h. A linear scratch was created across the cell monolayer using a sterile pipette tip. The experiment included four groups: MS, IL-33-MS, ST2/IL1RL1 + MS, and ST2/IL1RL1 + IL-33-MS, with ST2/IL1RL1 protein serving as an inhibitor of IL-33 signaling. Images of the scratch area were captured at 0, 24, and 48 h, and cell migration was quantified using ImageJ. The relative migration distance at 24 and 48 h was calculated based on the scratch width at 0 h.

## mRNA expression analysis and ELISA

Total RNA was extracted using TRIzol, and cDNA was synthesized via reverse transcription. Quantitative real-time PCR was conducted to determine gene expression levels, with *Gapdh* as the internal control. Relative expression was calculated using the 2^−ΔΔCT method. The released IL-33 was quantitated by ELISA. The capture and detection Abs for ELISA were obtained from BioLegend (San Diego, CA, USA)[25].

### Statistical analysis

Wound area measurements were analyzed using ImageJ software (Version 1.54k; URL: http://imagej.org). Statistical analyses and data visualization were performed using GraphPad Prism (Version 9.3.1; URL: https://www.graphpad.com). Data are presented as mean ± standard error of the mean (SEM). Student's t-test was used for comparisons between two groups, and one-way ANOVA was used for multiple group comparisons. A p-value < 0.05 was considered statistically significant.

## Results

### Optimization of microwave parameters

To clarify the therapeutic effects of microwave treatment alone, a full-thickness wound model was established on the dorsal skin of normal mice. Animals were divided into a control group and four microwave-treated groups (8 W 10 min, 10 W 10 min, 10 W 15 min, and 12 W 10 min). Among them, the 10 W 10 min group exhibited significant wound edge contraction by day 5, with a wound closure rate of 89.1 ± 1.1% by day 9 and 99.8 ± 0.2% by day 13, which was markedly higher than the control group (78.4 ± 5.8%, $p < 0.01$) and the other treatment groups. Histological analysis further supported these findings: H&E staining on day 7 showed well-aligned wound edges and orderly epidermal regeneration in the 10 W 10 min group, along with a significantly higher re-epithelialization rate compared to controls. On day 14, Masson's trichrome staining and quantitative analysis revealed a collagen volume fraction 1.37 ± 0.09 times greater than that of the control group ($p < 0.05$), indicating enhanced collagen deposition. Additionally, immunofluorescence analysis on day 7 demonstrated significantly increased $CD31^+$ neovascular density and $\alpha\text{-SMA}^+$ myofibroblast proportion (31.9 ± 6.8% and 57.0 ± 3.1%, respectively; $p < 0.01$). Collectively, these results indicate that microwave therapy at 10 W for 10 min effectively promotes wound healing in normal mice by accelerating epidermal regeneration, collagen remodeling, and angiogenesis.

### Microwave therapy promotes diabetic wound healing

Based on the optimal parameters established in normal mice, the 10 W 10 min microwave setting was applied to a diabetic wound model. Following successful wound induction (Fig. 2A–B), microwave treatment significantly accelerated healing, with the DM + 10 W 10 min group exhibiting markedly higher wound contraction rates on days 1, 5, 9, and 13 compared to the untreated DM group (Fig. 2C–E). On day 7, H&E staining revealed disrupted epidermal continuity and prominent inflammatory infiltration in the DM group, whereas the microwave-treated group displayed intact epidermal coverage, reduced inflammation, and well-organized tissue structure (Fig. 2F). Quantitative analysis confirmed significantly enhanced epithelial migration in the treated group ($p < 0.01$; Fig. 2G). On day 14, Masson's staining showed denser, more organized collagen fibers in the DM + 10 W 10 min group, with a 1.37 ± 0.09-fold increase over controls (Fig. 2H–I). Additionally, $CD31^+$ neovascular density and $\alpha\text{-SMA}^+$ myofibroblast proportion were significantly increased to 67.3 ± 16.9% and 69.2 ± 12.4%, respectively ($p < 0.05$; Fig. 2J–L, O), and qPCR revealed upregulation of *Vegf* and *vWF* expression (Fig. 2M–N). Furthermore, immunofluorescence and qPCR analyses demonstrated elevated type I collagen expression and increased mRNA levels of *Col3a1* and *Fn1* in the microwave-treated group ($p < 0.05$; Fig. 2P–U), indicating enhanced extracellular matrix remodeling. These findings collectively suggest that microwave therapy effectively promotes re-epithelialization, angiogenesis, and matrix reconstruction in diabetic wounds.

### Microwave-induced IL-33 upregulation promotes macrophage M2 polarization and enhances diabetic wound healing

Immunofluorescence and qPCR analyses demonstrated that microwave treatment significantly upregulated IL-33 expression in diabetic wound tissues (Fig. 3A, D and M). IL-33 was found in both keratinocytes ($Krt14^+$) and macrophages ($F4/80^+$), with co-localization more prominent in macrophages—1.34-fold higher than in keratinocytes—indicating that macrophages are the primary source of IL-33 (Fig. 3B–C and E–F). In the DM + 10 W 10 min group, co-expression of M2 markers CD206 and F4/80 increased, whereas co-expression of M1 markers iNOS and F4/80 decreased (Fig. 3G–J). This phenotypic shift was further supported by qPCR, which showed significant upregulation of M2-associated genes *YM1* and *IL-4* and downregulation of M1-associated genes *Tnf-α*, *iNOS*, and *IL-6* ($p < 0.01$; Fig. 3K–P). These findings suggest that microwave therapy enhances IL-33 expression in diabetic wounds, thereby promoting macrophage polarization from the M1 to M2 phenotype, modulating the inflammatory microenvironment, and contributing to improved wound repair.

### Microwave therapy has no restorative effect in ST2-deficient mice

To confirm the essential role of the IL-33/ST2 signaling pathway, wound healing outcomes were compared between wild-type (WT) and ST2-deficient ($ST2^{-/-}$) mice following microwave treatment. $ST2^{-/-}$ mice exhibited delayed wound healing, larger scar areas, and no significant improvement after microwave exposure (Fig. 4A–C). Histological analysis revealed impaired epidermal regeneration, a disorganized dermal structure, and irregular collagen arrangement in $ST2^{-/-}$ mice (Fig. 4D–G). Immunofluorescence analysis showed markedly reduced expression of CD31 and α-SMA compared to WT controls (Fig. 4H–K). qPCR analysis demonstrated decreased expression of angiogenic markers VEGF and vWF in $ST2^{-/-}$ mice, with no observable enhancement following microwave treatment (Fig. 4P–Q). Furthermore, *ST2* mRNA expression was significantly downregulated in both $ST2^{-/-}$ and $ST2^{-/-}$+MW groups relative to WT (Fig. 4L), while M2 marker *YM1* was decreased and M1-related gene *IL-6* was elevated (Fig. 4O and N); *IL-33* expression showed no significant differences (Fig. 4M). These results indicate that ST2 deficiency abolishes the therapeutic effects of microwave treatment, underscoring the critical role of the IL-33/ST2 axis in mediating microwave-induced wound healing responses.

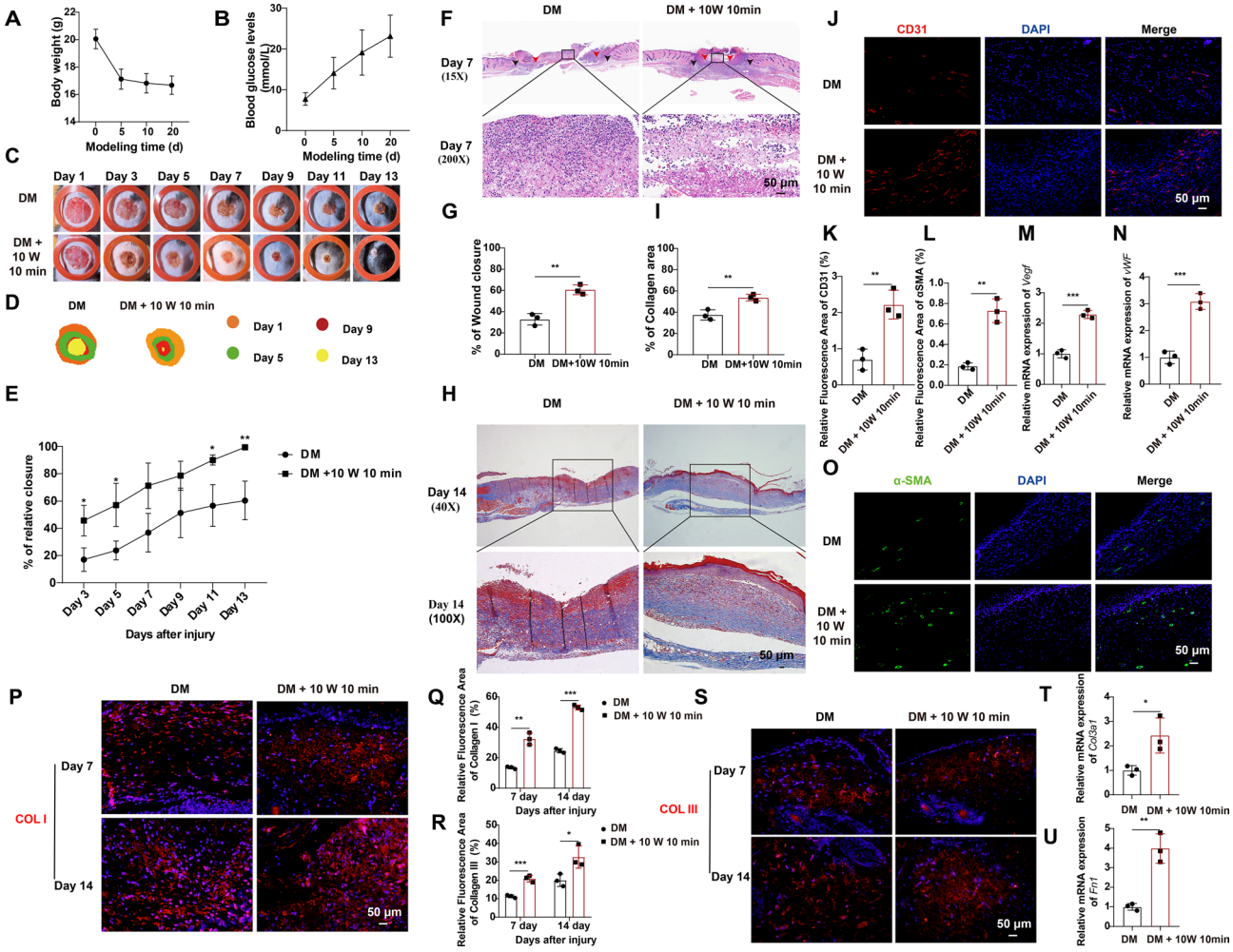


**Fig. 2**. Microwave therapy promotes wound healing in diabetic mice. (**A–B**) Changes in body weight of mice after streptozotocin induction. (**C**) Representative images of wound healing in diabetic mice on days 1, 3, 5, 7, 9, 11, and 13. (**D**) Overlaid wound contours at different time points for each group. (**E**) Quantitative analysis of wound closure rates. (**F**) H&E staining on day 7 (black arrows indicate wound edges; red arrows indicate epidermis). (**G**) Quantification of epidermal regeneration rate. (**H**) Masson's trichrome staining on day 14. $n = 3$ per group. (**I**) Quantitative analysis of collagen volume fraction. $n = 3$ per group. (J) CD31 immunofluorescence staining (red) on day 7. (**K**) Percentage of CD31-positive fluorescence area. $n = 3$ per group (**L**) Percentage of α-SMA-positive fluorescence area. $n = 3$ per group (**M–N**) mRNA expression levels of *Vegf* and *vWF*. $n = 3$ per group. (**O**) α-SMA immunofluorescence staining (green) on day 7. $n = 3$ per group. (**P**) Collagen I immunofluorescence staining (red) on days 7 and 14. (**Q–R**) Quantitative analysis of fluorescence-positive areas for Collagen I and III. $n = 3$ per group. (**S**) Collagen III immunofluorescence staining (red) on days 7 and 14. (**T–U**) Gene expression levels of *Col3a1* and *Fn1*. $n = 3$ per group. (ns = not significant ($p > 0.05$); $^{*}p < 0.05$; $^{**}p < 0.01$; $^{***}p < 0.001$).

## In vitro effects of microwave on macrophages and keratinocytes

In vitro experiments exploring various microwave intensities and durations identified 8 W for 10 min as the optimal condition for cellular responses (Fig. 5A–J and Figure S1). Under this setting, IL-33 expression was significantly elevated in both RAW264.7 macrophages and HaCaT keratinocytes, with higher levels observed in macrophages, suggesting that macrophages are the primary responsive cell type. Functionally, IL-33-enriched macrophage supernatant (IL-33-MS) significantly upregulated M2 markers *IL-4* and *YM1*, while downregulating M1 markers *iNOS* and *Tnf-α* in macrophages (Fig. 5N–Q), indicating potent anti-inflammatory effects. In scratch assays, IL-33-MS notably enhanced HaCaT cell migration, an effect that was attenuated by the addition of ST2/IL1RL1 recombinant protein—an IL-33 pathway inhibitor—demonstrating that IL-33/ST2 signaling is critical for keratinocyte migration (Fig. 5K–M).

## Effects of IL-33-MS on wound healing in ST2-deficient mice

To further elucidate the role of IL-33 in wound repair, IL-33-MS was applied topically to wounds in WT and $ST2^{-/-}$ mice. IL-33-MS significantly accelerated healing in WT mice but had no effect in $ST2^{-/-}$ mice (Fig. 6A–C).H&E staining showed intact epidermis and organized tissue in the IL-33-MS group, while $ST2^{-/-}$ and $ST2^{-/-}$+IL-33-

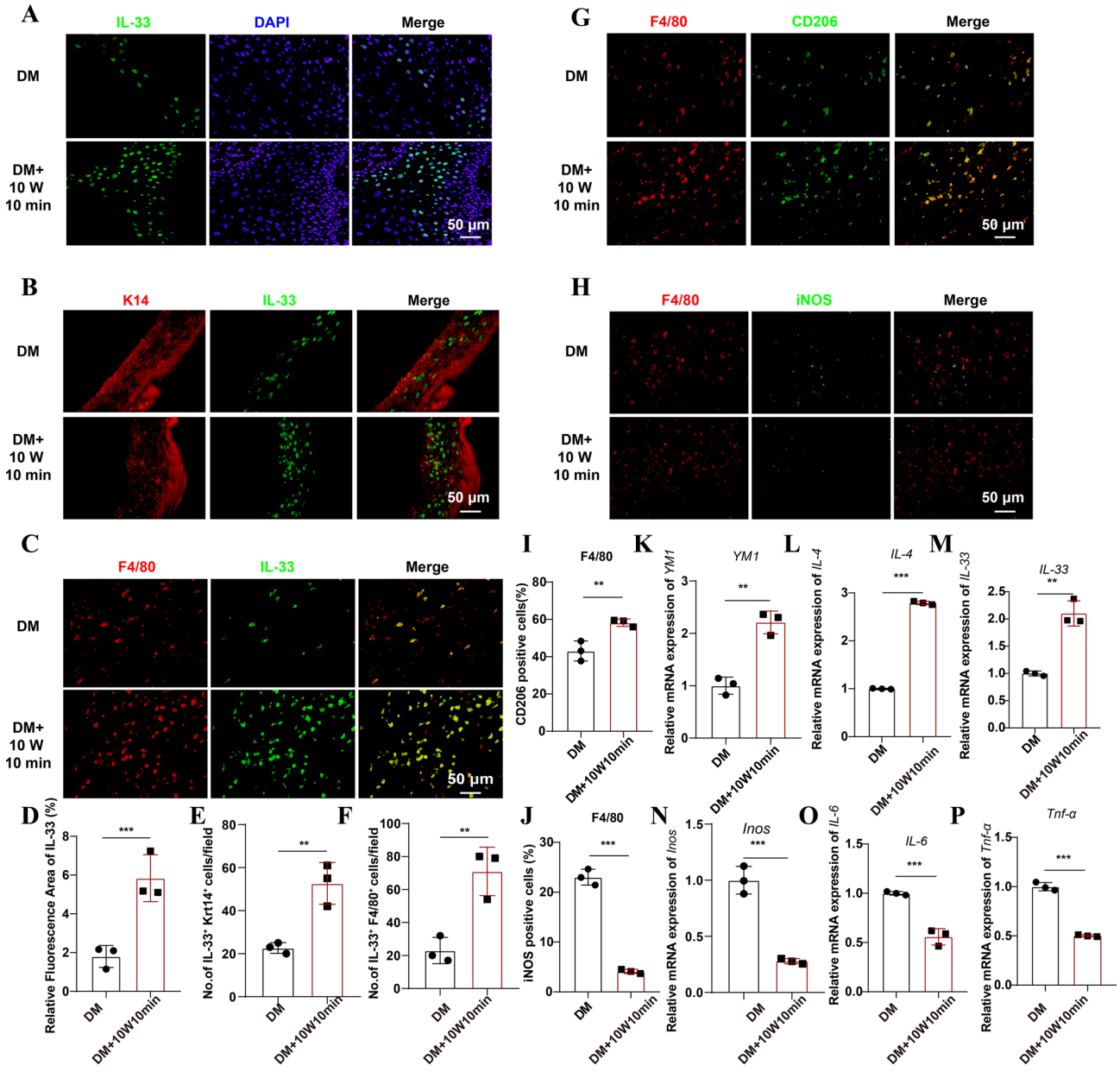


**Fig. 3**. Microwave therapy upregulates IL-33 expression, promotes macrophage M2 polarization, and enhances diabetic wound healing. (**A**) IL-33 expression (green) in diabetic mouse skin on day 7. (**B–C**) Co-immunofluorescence staining of IL-33 with Krt14 (red) and F4/80 (red), respectively. (**D**) Quantification of IL-33-positive fluorescence area. (**E–F**) Quantification of IL-33$^+$/Krt14$^+$ and IL-33$^+$/F4/80$^+$ double-positive cells. (**G–H**) Co-expression images of CD206 (green) with F4/80 and iNOS (green) with F4/80. (**I–J**) Percentage of CD206$^+$ and iNOS$^+$ cells. $n = 3$ per group. (**K–P**) mRNA expression levels of *YM1*, *IL-4*, *IL-33*, *iNOS*, *IL-6*, and *Tnf-α*. $n = 3$ per group. (ns = not significant ($p > 0.05$); $^*p < 0.05$; $^{**}p < 0.01$; $^{***}p < 0.001$).

MS groups displayed disrupted epidermis and disorganized structure (Fig. 6D). On day 14, Masson staining and quantitative analysis showed the highest collagen expression in the IL-33-MS group; collagen levels were significantly lower in ST2$^{-/-}$ mice, regardless of treatment (Fig. 6E–F). Immunofluorescence revealed markedly increased CD31 and α-SMA expression in the IL-33-MS group, which were reduced in the ST2$^{-/-}$+IL-33-MS group (Fig. 6G–J).These results confirm that the reparative effects of IL-33 depend on the ST2 receptor, further supporting the key role of the IL-33/ST2 pathway in mediating the benefits of microwave therapy in diabetic wound healing.

## Discussion

Delayed wound healing in diabetes is a multifactorial pathological process involving persistent inflammation, dysregulated immune cell function, impaired neovascularization, and disrupted extracellular matrix (ECM) remodeling[26–28]. In this study, we demonstrated that microwave physiotherapy significantly enhances wound

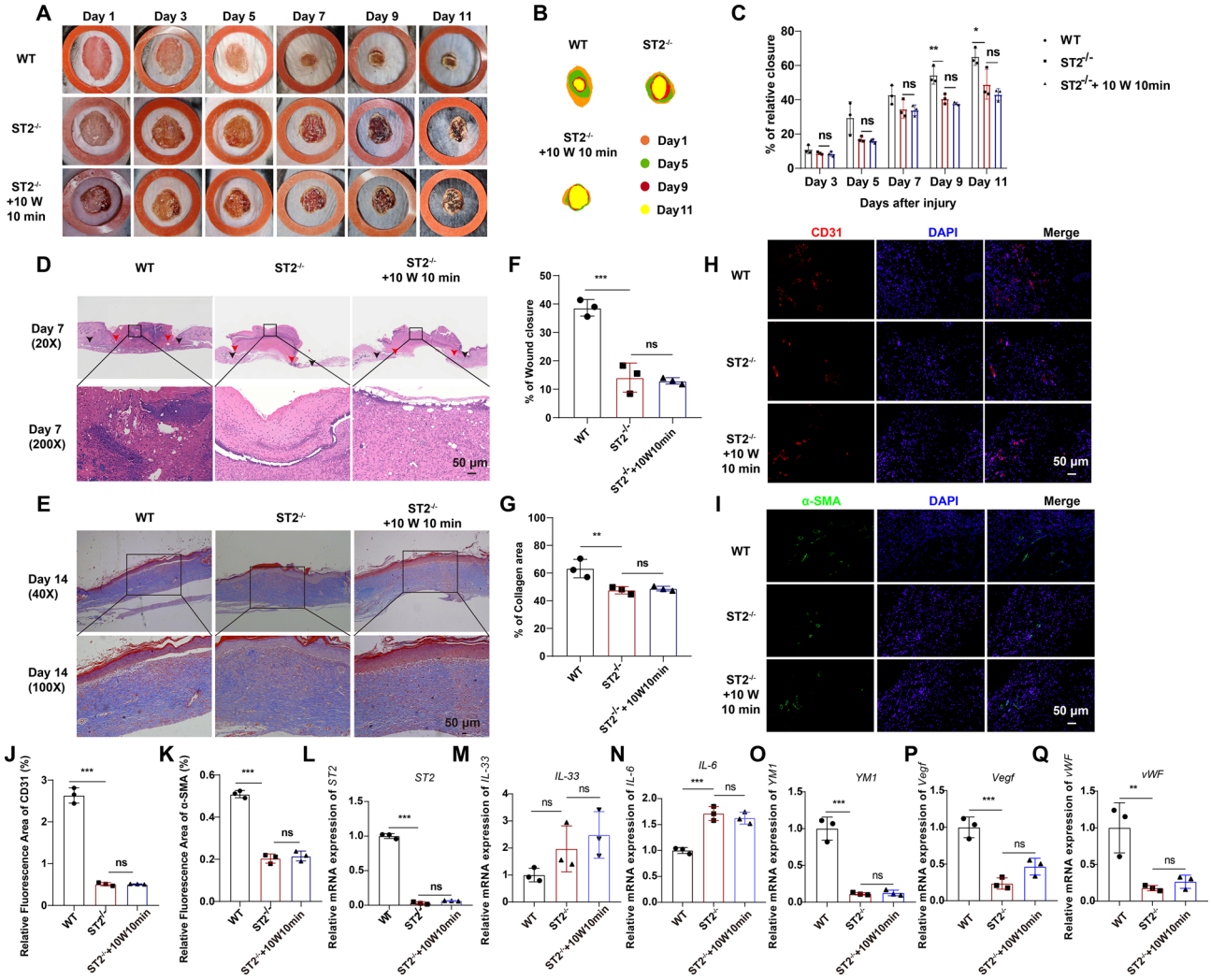


**Fig. 4**. Loss of microwave-induced pro-healing effects in ST2-deficient mice. (**A**) Representative images of wound healing on days 1, 3, 5, 7, 9, and 11 in each group. $n = 3$ per group. (**B**) Overlaid wound outlines at different time points. (**C**) Quantitative analysis of wound closure rates. $n = 3$ per group. (**D**) H&E staining of wound tissues on day 7. (**E**) Masson's trichrome staining on day 14. (**F**) Quantification of epidermal regeneration rate. $n = 3$ per group. (**G**) Collagen volume fraction analysis. $n = 3$ per group. (**H–I**) Immunofluorescence staining of CD31 (red) and α-SMA (green) on day 7. (**J–K**) Quantitative analysis of $CD31^+$ and $\alpha\text{-}SMA^+$ fluorescence area percentages. $n = 3$ per group. (L–Q) mRNA expression levels of *ST2*, *IL-33*, *IL-6*, *YM1*, *Vegf*, and *vWF*. $n = 3$ per group. (ns = not significant ($p > 0.05$); $^*p < 0.05$; $^{**}p < 0.01$; $^{***}p < 0.001$).

healing in diabetic mice, with optimal effects observed at a setting of 10 W for 10 min. This intervention led to accelerated epithelial regeneration, increased collagen deposition, and improved neovascularization. These benefits were associated with the upregulation of IL-33 and subsequent activation of the IL-33/ST2 signaling pathway, highlighting a novel immunomodulatory mechanism in physical therapy-mediated wound repair. This work extends, to some extent, the role of microwave therapy in disease. Previous studies have indicated that microwave ablation can modulate immune responses to influence tumor progression[29]. A key finding of the present study is the identification of IL-33 as a central mediator of the microwave-induced repair response. Indeed, IL-33 has recently attracted considerable attention as a critical regulator of tissue homeostasis and repair[30]. We found that IL-33 is predominantly produced by macrophages within the diabetic wound microenvironment and is significantly upregulated following microwave treatment. This cytokine functions as an "alarmin" and initiates downstream immune responses through binding to its receptor, ST2[31]. Consistent with previous reports[32,33], our data confirm that IL-33 expression is essential for wound repair under pathological conditions, with its effects primarily mediated by ST2-expressing target cells.

Anti-inflammatory interventions are recognized as important strategies to promote diabetic wound healing[34]. Specifically, inhibition of the inflammatory response can be achieved by increasing the ratio of M2- to M1-polarized macrophages, thereby facilitating wound repair in diabetes[35]. We demonstrated that microwave-induced IL-33 promotes polarization toward the M2 macrophage phenotype, characterized by increased expression of CD206, IL-4, and YM1, while concurrently reducing pro-inflammatory M1 markers such as iNOS,

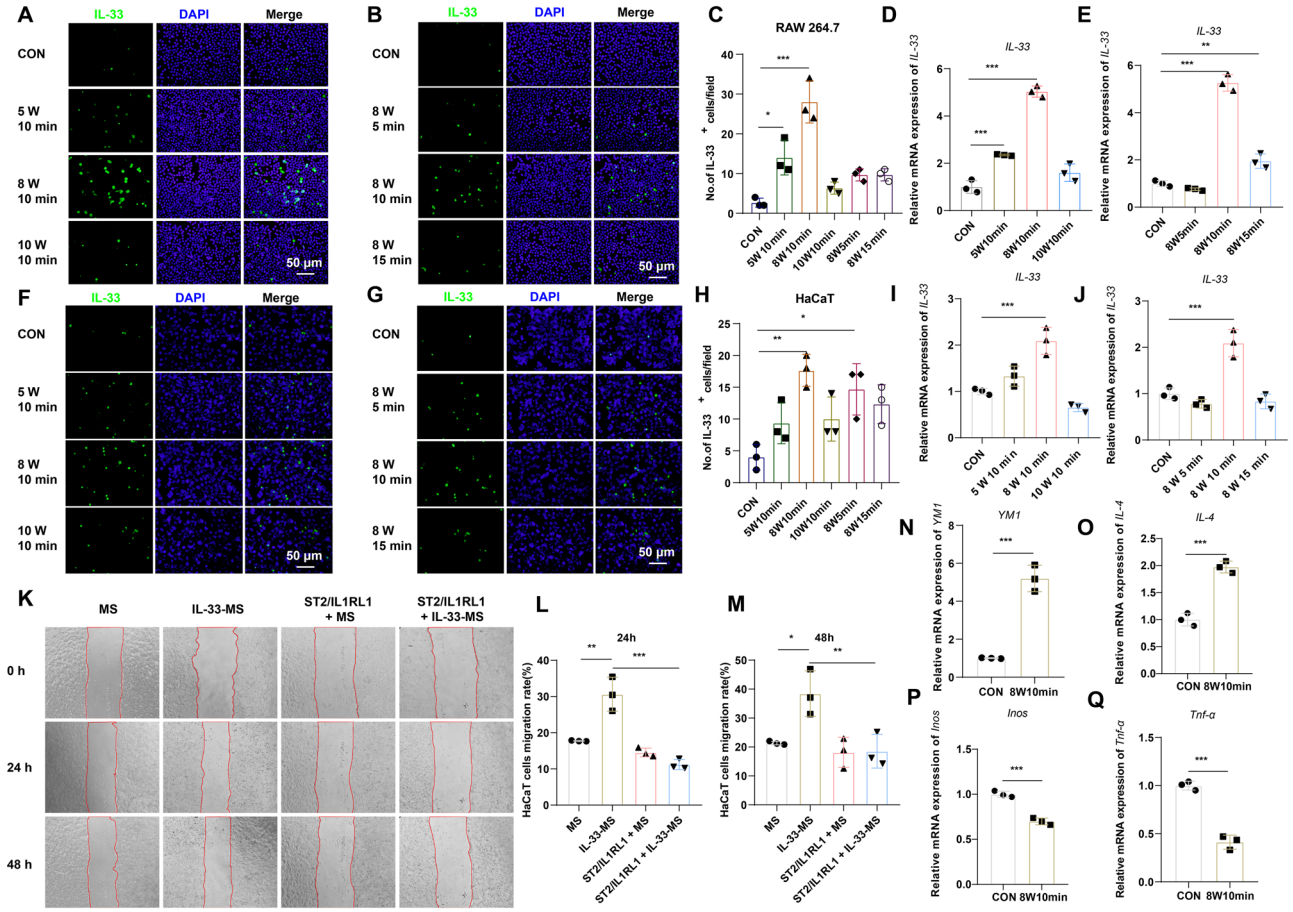


**Fig. 5**. In vitro validation of microwave effects on macrophages and keratinocytes. (**A–B**) IL-33 expression (green) in RAW264.7 macrophages after microwave treatment with different power levels and durations. (**C**) Quantification of IL-33⁺ macrophages per field in each group. (**D–E**) mRNA expression levels of *IL-33* in macrophages under various conditions. (**F–G**) IL-33 expression (green) in HaCaT keratinocytes under different microwave conditions.(H) Quantification of IL-33⁺ HaCaT cells per field in each group. (**I–J**) mRNA expression levels of *IL-33* in HaCaT cells. (**K**) Scratch assay images showing HaCaT wound closure after treatment with RAW macrophage supernatants. (**L–M**) Quantitative analysis of HaCaT cell migration rates at 24 h and 48 h. (**N–Q**) mRNA expression levels of *YM1*, *IL-4*, *iNOS*, and *Tnf-α* in RAW264.7 macrophages following microwave treatment.(ns = not significant ($p > 0.05$); *$p < 0.05$; **$p < 0.01$; ***$p < 0.001$).

Tnf-α, and IL-6. This highlights the regulatory role of macrophage polarization in modulating the inflammatory milieu. M2 macrophages play a critical role in wound healing by secreting anti-inflammatory cytokines, promoting angiogenesis, and facilitating fibroblast activation and extracellular matrix (ECM) synthesis[14,24]. Our in vitro and in vivo data consistently support that the shift toward M2 polarization contributes to the reactivation of the repair phase in diabetic wounds. This provides a mechanistic explanation for the improved histological outcomes observed with microwave therapy. Although previous studies have demonstrated that microwave therapy can enhance wound repair[36] and accelerate healing in both septic and sterile rabbit wound models[37], the molecular mechanisms underlying its reparative effects remain largely unexplored.

Our study confirms the critical role of IL-33/ST2 signaling in microwave-promoted wound healing. Using ST2-deficient mice, we found that microwave treatment failed to induce wound repair in the absence of this receptor. These mice exhibited impaired re-epithelialization, disorganized collagen architecture, and reduced expression of CD31 and α-SMA, indicating compromised angiogenesis and myofibroblast activation. Furthermore, local administration of IL-33-enriched macrophage supernatant (IL-33-MS) accelerated wound healing in wild-type mice but had no effect in ST2-deficient animals, further validating the specificity and indispensability of this signaling axis. The paracrine effect of M2 macrophages was also supported by scratch assays, where IL-33-MS significantly enhanced keratinocyte migration. This effect was attenuated by an ST2/IL1RL1 inhibitor, suggesting that IL-33 secreted from polarized M2 macrophages not only alters the immune microenvironment but also directly stimulates epithelial cell migration. Such dual action reinforces the central role of macrophage-derived IL-33 in coordinating cellular crosstalk during tissue regeneration. It is noteworthy that in previous experimental studies on wound healing, the emergence of M2 macrophage polarization was primarily attributed to the paracrine effects of stem cells[38–40]. Our study extends this understanding by demonstrating that M2 macrophages themselves can act as initiators, driving downstream effector cells to promote wound repair.

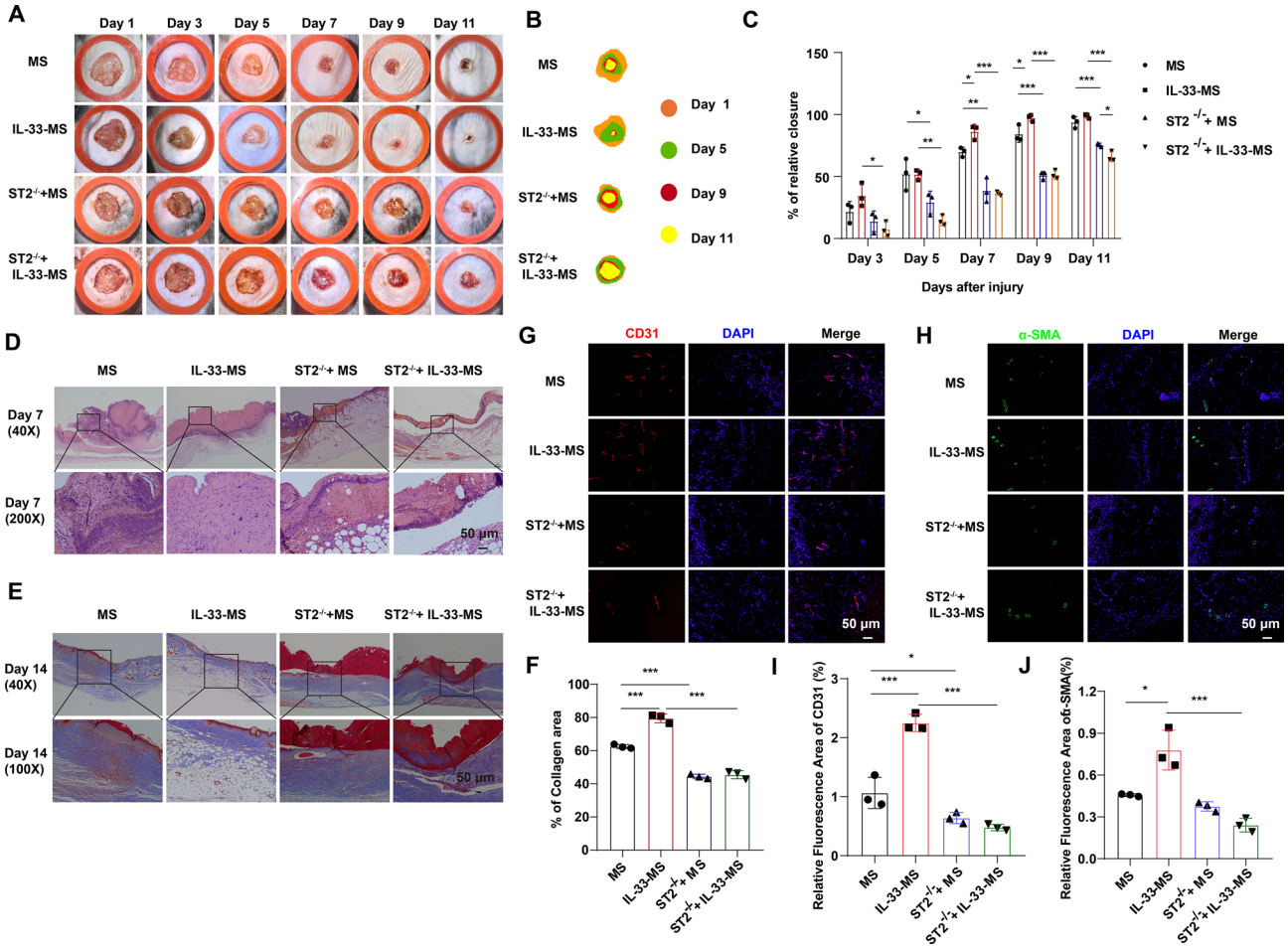


**Fig. 6**. IL-33-enriched macrophage supernatant (IL-33-MS) promotes wound healing in WT mice. (**A**) Representative images of wound healing on days 1, 3, 5, 7, 9, and 11 in each group. (**B**) Overlaid wound contours illustrating the healing progression in different groups. (C) Quantitative analysis of wound closure rates. $n = 3$ per group. (**D**) H&E staining on day 7. (**E**) Masson's trichrome staining on day 14. (**F**) Quantitative analysis of collagen volume fraction. $n = 3$ per group. (**G–H**) Immunofluorescence staining of CD31 (red) and α-SMA (green) on day 7. (**I–J**) Quantification of $CD31^+$ and $\alpha\text{-SMA}^+$ fluorescence area percentages. $n = 3$ per group. (ns = not significant ($p > 0.05$); $^*p < 0.05$; $^{**}p < 0.01$; $^{***}p < 0.001$).

In summary, our study reveals a novel mechanism by which microwave therapy enhances diabetic wound healing through IL-33/ST2-driven M2 macrophage polarization. By alleviating chronic inflammation, promoting angiogenesis, and stimulating epithelial remodeling, microwave therapy may addresses several pathological bottlenecks in diabetic wound repair. Future studies should explore the downstream effectors of IL-33/ST2 signaling, including potential interactions with fibroblasts and stem cells, and assess the safety and efficacy of this strategy in preclinical models that more closely mimic human wound conditions.

## Data availability

All analyses conducted in the article used publicly available data. Detailed statements can be found in the original articles. The datasets generated and analysed during the current study are included in this article.

Received: 28 June 2025; Accepted: 24 September 2025
Published online: 30 October 2025

## References

1. Sugandh, F. et al. Advances in the management of diabetes mellitus: A focus on personalized medicine. *Cureus* **15**, e43697. https://doi.org/10.7759/cureus.43697 (2023).
2. Sun, H. et al. IDF diabetes atlas: Global, regional and country-level diabetes prevalence estimates for 2021 and projections for 2045. *Diabetes Res. Clin. Pract.* **183**, 109119. https://doi.org/10.1016/j.diabres.2021.109119 (2022).
3. Song, J., Wu, Y., Chen, Y., Sun, X. & Zhang, Z. Epigenetic regulatory mechanism of macrophage polarization in diabetic wound healing (Review). *Mol. Med. Rep.* **31** https://doi.org/10.3892/mmr.2024.13367 (2025).
4. Doğruel, H., Aydemir, M. & Balci, M. K. Management of diabetic foot ulcers and the challenging points: an endocrine view. *World J. Diabetes*. **13**, 27–36. https://doi.org/10.4239/wjd.v13.i1.27 (2022).

5. Rayman, G. et al. Guidelines on use of interventions to enhance healing of chronic foot ulcers in diabetes (IWGDF 2019 update). *Diab./Metab. Res. Rev.* **36** (Suppl 1), e3283. https://doi.org/10.1002/dmrr.3283 (2020).
6. Armstrong, D. G., Tan, T. W., Boulton, A. J. M. & Bus, S. A. Diabetic foot ulcers: A review. *JAMA* **330**, 62–75. https://doi.org/10.1001/jama.2023.10578 (2023).
7. Schramm, J. M., Warner, D., Hardesty, R. A. & Oberg, K. C. A unique combination of infrared and microwave radiation accelerates wound healing. *Plast. Reconstr. Surg.* **111**, 258–266 (2003).
8. Albarqi, H. A. et al. Microwave-Assisted physically Cross-Linked Chitosan-Sodium alginate hydrogel membrane doped with Curcumin as a novel wound healing platform. *AAPS PharmSciTech*. **23**, 72. https://doi.org/10.1208/s12249-022-02222-y (2022).
9. Basit, H. M. et al. Microwave enabled physically cross linked sodium alginate and pectin film and their application in combination with modified Chitosan-Curcumin Nanoparticles. A novel strategy for 2nd degree burns wound healing in animals. *Polym. (Basel)*. 13. https://doi.org/10.3390/polym13162716 (2021).
10. Eskandari, S. et al. Efficacy of microwave and infrared radiation in the treatment of the skin lesions caused by leishmania major in an animal model. *Iran. J. Public. Health*. **41**, 80–83 (2012).
11. Singh, B. & Bate, L. A. Responses of pulmonary intravascular macrophages to 915-MHz microwave radiation: ultrastructural and cytochemical study. *Anat. Rec.* **246**, 343–355 (1996).
12. Lertpatipanpong, P. et al. Effect of cold atmospheric microwave plasma (CAMP) on wound healing in canine keratinocytes. *Front. Cell. Dev. Biol.* **11**, 1105692. https://doi.org/10.3389/fcell.2023.1105692 (2023).
13. Yoo, J., Kang, Y. H., Baek, S. J. & Hwang, C. Y. Application of cold atmospheric microwave plasma as an adjunct therapy for wound healing in dogs and cats. *J. Vet. Sci.* **24**, e56. https://doi.org/10.4142/jvs.23067 (2023).
14. Zhou, X., Guo, Y. L., Xu, C., Wang, J. & Macrophages Key players in diabetic wound healing. *World J. Diabetes*. **15**, 2177–2181. https://doi.org/10.4239/wjd.v15.i11.2177 (2024).
15. Barman, P. K. & Koh, T. J. Macrophage dysregulation and impaired skin wound healing in diabetes. *Front. Cell. Dev. Biol.* **8**, 528. https://doi.org/10.3389/fcell.2020.00528 (2020).
16. He, P. Y. et al. Interleukin-33/serum stimulation-2 pathway: regulatory mechanisms and emerging implications in immune and inflammatory diseases. *Cytokine Growth Factor. Rev.* **76**, 112–126. https://doi.org/10.1016/j.cytogfr.2023.12.001 (2024).
17. Molofsky, A. B., Savage, A. K. & Locksley, R. M. Interleukin-33 in tissue Homeostasis, Injury, and inflammation. *Immunity* **42**, 1005–1019. https://doi.org/10.1016/j.immuni.2015.06.006 (2015).
18. Wang, Y. et al. Exosomes from adipose-derived stem cells accelerate wound healing by increasing the release of IL-33 from macrophages. *Stem Cell. Res. Ther.* **16**, 80. https://doi.org/10.1186/s13287-025-04203-x (2025).
19. Yin, H. et al. IL-33 accelerates cutaneous wound healing involved in upregulation of alternatively activated macrophages. *Mol. Immunol.* **56**, 347–353. https://doi.org/10.1016/j.molimm.2013.05.225 (2013).
20. Fan, X. et al. The promoting effect of animal bioactive proteins and peptide components on wound healing: A review. *Int. J. Mol. Sci.* **25** https://doi.org/10.3390/ijms252312561 (2024).
21. Xu, R. et al. IL-33/ST2 induces macrophage-dependent ROS production and TRPA1 activation that mediate pain-like responses by skin incision in mice. *Theranostics* **14**, 5281–5302. https://doi.org/10.7150/thno.97856 (2024).
22. Lou, J. et al. Diabetes exacerbates periodontitis by disrupting IL-33-mediated interaction between periodontal ligament fibroblasts and macrophages. *Int. Immunopharmacol.* **147**, 113896. https://doi.org/10.1016/j.intimp.2024.113896 (2025).
23. Shakerian, L. et al. IL-33/ST2 axis in autoimmune disease. *Cytokine* **158**, 156015. https://doi.org/10.1016/j.cyto.2022.156015 (2022).
24. He, R. et al. IL-33 improves wound healing through enhanced M2 macrophage polarization in diabetic mice. *Mol. Immunol.* **90**, 42–49. https://doi.org/10.1016/j.molimm.2017.06.249 (2017).
25. Hiraide, S., Yanagawa, Y. & Iizuka, K. Tranilast inhibits interleukin-33 production by macrophages. *Eur. J. Pharmacol.* **818**, 235–240. https://doi.org/10.1016/j.ejphar.2017.10.057 (2018).
26. Ahmed, A. S. & Antonsen, E. L. Immune and vascular dysfunction in diabetic wound healing. *J. Wound Care*. **25**, S35–S46. https://doi.org/10.12968/jowc.2016.25.Sup7.S35 (2016).
27. Yang, P. et al. Compromised wound healing in ischemic type 2 diabetic rats. *PLoS One*. **11**, e0152068. https://doi.org/10.1371/journal.pone.0152068 (2016).
28. Pradhan, L., Nabzdyk, C., Andersen, N. D., LoGerfo, F. W. & Veves, A. Inflammation and neuropeptides: the connection in diabetic wound healing. *Expert Rev. Mol. Med.* **11**, e2. https://doi.org/10.1017/S1462399409000945 (2009).
29. Wu, S. et al. Tregs ST2 deficiency enhances the abscopal anti-tumor response induced by microwave ablation. *Int. Immunopharmacol.* **143**, 113330. https://doi.org/10.1016/j.intimp.2024.113330 (2024).
30. Cayrol, C. & Girard, J. P. Interleukin-33 (IL-33): A critical review of its biology and the mechanisms involved in its release as a potent extracellular cytokine. *Cytokine* **156**, 155891. https://doi.org/10.1016/j.cyto.2022.155891 (2022).
31. Lee, J. S., Seppanen, E., Patel, J., Rodero, M. P. & Khosrotehrani, K. ST2 receptor invalidation maintains wound inflammation, delays healing and increases fibrosis. *Exp. Dermatol.* **25**, 71–74. https://doi.org/10.1111/exd.12833 (2016).
32. Lopetuso, L. R., Scaldaferri, F. & Pizarro, T. T. Emerging role of the Interleukin (IL)-33/ST2 axis in gut mucosal wound healing and fibrosis. *Fibrogenesis Tissue Repair.* **5**, 18. https://doi.org/10.1186/1755-1536-5-18 (2012).
33. Gao, Y. et al. Extended characterization of IL-33/ST2 as a predictor for wound age determination in skin wound tissue samples of humans and mice. *Int. J. Legal Med.* **137**, 1287–1299. https://doi.org/10.1007/s00414-023-03025-x (2023).
34. Zhu, S. et al. Microenvironment responsive nanocomposite hydrogel with NIR photothermal therapy, vascularization and anti-inflammation for diabetic infected wound healing. *Bioact Mater.* **26**, 306–320. https://doi.org/10.1016/j.bioactmat.2023.03.005 (2023).
35. Liu, W. et al. Melatonin-stimulated MSC-derived exosomes improve diabetic wound healing through regulating macrophage M1 and M2 polarization by targeting the PTEN/AKT pathway. *Stem Cell. Res. Ther.* **11**, 259. https://doi.org/10.1186/s13287-020-01756-x (2020).
36. Ye, D. et al. Effects of low-dose microwave on healing of fractures with titanium alloy internal fixation: an experimental study in a rabbit model. *PLoS One*. **8**, e75756. https://doi.org/10.1371/journal.pone.0075756 (2013).
37. Korpan, N. N., Resch, K. L. & Kokoschinegg, P. Continuous microwave enhances the healing process of septic and aseptic wounds in rabbits. *J. Surg. Res.* **57**, 667–671. https://doi.org/10.1006/jsre.1994.1198 (1994).
38. Su, X. et al. Fibrous scaffolds loaded with BMSC-derived apoptotic vesicles promote wound healing by inducing macrophage polarization. *Genes Dis.* **12**, 101388. https://doi.org/10.1016/j.gendis.2024.101388 (2025).
39. Liu, C. et al. Mesenchymal stromal cells pretreated with Proinflammatory cytokines enhance skin wound healing via IL-6-dependent M2 polarization. *Stem Cell. Res. Ther.* **13**, 414. https://doi.org/10.1186/s13287-022-02934-9 (2022).
40. He, X. et al. MSC-Derived Exosome Promotes M2 Polarization and Enhances Cutaneous Wound Healing. *Stem Cells Int* 7132708, (2019). https://doi.org/10.1155/2019/7132708 (2019).


## Acknowledgements

This work was supported by the Guangzhou Science and Technology Bureau Project (Grant No. 2023A03J0972) and the Key Area Project of General Universities in Guangdong Province (Grant No. 2024ZDZX2080).

## Author contributions

HMX, HXL, LT, YH, and HRG conceived and designed the experiments. HMX, HXL, and LT performed the experiments and drafted the manuscript. YQ, ZYF, WYX, ZYN, and PSF provided technical support and assisted in completing the study. LYM, LZM, and PSF conducted data analysis. YQ, WYX, and ZYF contributed to manuscript review and project coordination. LT, YH, and HRG provided resources. HRG and YH supervised the entire project. All authors read and approved the final version of the manuscript.

## Funding

This work was supported by the Guangzhou Science and Technology Bureau Project (Grant No. 2023A03J0972) and the Key Area Project of General Universities in Guangdong Province (Grant No. 2024ZDZX2080).

## Declarations

## Competing interests

The authors declare no competing interests.

## Ethics statement

The experimental protocol met the ethical requirements of animal welfare, and the animal experiment was approved through the ethical review of animal experiment by (Acceptance number: GDPULAC2024104).

## Additional information

**Correspondence** and requests for materials should be addressed to H.Y. or R.H.